Original Research Paper

Sequentially releasing self-healing hydrogel fabricated with TGFβ3-microspheres and bFGF to facilitate rat alveolar bone defect repair

Fenglin Yu [a,b,c,#], Dezhi Geng [a,b,c,#], Zhanpeng Kuang [a,b,c], Shiyi Huang [a,b,c], Yating Cheng [a,b,c], Yini Chen [a,b,c], Fang Leng [c], Yu Bei [c], Yueping Zhao [d], Qingxia Tang [d], Yadong Huang [a,b,c], Qi Xiang [a,b,c,*]

[a] Department of Cell Biology, College of Life Science and Technology, Jinan University, Guangzhou 510632, China
[b] Guangdong Province Key Laboratory of Bioengineering Medicine, Jinan University, Guangzhou 510632, China
[c] Biopharmaceutical R&D Center of Jinan University, Guangzhou 510632, China
[d] Department of Stomatology, Jinan University Medical College, Guangzhou 510632, China

ARTICLE INFO

ABSTRACT

Resorption and loss of alveolar bone leads to oral dysfunction and loss of natural or implant teeth. Biomimetic delivery of growth factors based on stem cell recruitment and osteogenic differentiation, as the key steps in natural alveolar bone regenerative process, has been an area of intense research in recent years. A mesoporous self-healing hydrogel (DFH) with basic fibroblast growth factor (bFGF) entrapment and transforming growth factor $\beta3$ (TGFβ3) - loaded chitosan microspheres (CMs) was developed. The formulation was optimized by multiple tests of self-healing, in-bottle inversion, SEM, rheological, swelling rate and *in vitro* degradation. *In vitro* tubule formation assays, cell migration assays, and osteogenic differentiation assays confirmed the ability of DFH to promote blood vessels, recruit stem cells, and promote osteogenic differentiation. The optimum DFH formula is 0.05 ml 4Arm-PEG-DF (20%) added to 1 ml CsGlu (2%) containing bFGF (80 ng) and TGFβ3-microspheres (5 mg). The results of *in vitro* release studied by Elisa kit, indicated an 95% release of bFGF in 7 d and long-term sustained release of TGFβ3. For alveolar defects rat models, the expression levels of CD29 and CD45, the bone volume fraction, trabecular number, and trabecular thickness of new bone monitored by Micro-CT in DFH treatment groups were significantly higher than others (*$P < 0.05$, *vs* Model). HE and Masson staining show the same results. In conclusion, DFH is a design of bionic alveolar remodelling microenvironment, that is in

* Corresponding author.
  E-mail address: txiangqi@jnu.edu.cn (Q. Xiang).
# These authors contributed equally to the work.
  Peer review under responsibility of Shenyang Pharmaceutical University.

early time microvessels formed by bFGF provide nutritious to recruited endogenous stem cells, then TGFβ3 slowly released speed up the process of new bones formation to common facilitate rat alveolar defect repair. The DFH with higher regenerative efficiency dovetails nicely with great demand due to the requirement of complicated biological processes.

1. Introduction

Periodontal disease is one of the most common diseases of the oral cavity. It induces plaque accumulation, dysbacteriosis, periodontal pocket formation, gingival recession, tissue destruction, and loss of the alveolar bone, eventually leading to tooth loss. In fact, it is one of the primary reasons behind tooth loss in adults [1,2]. Epidemiological studies have revealed that the incidence of periodontal disease is as high as 90% [3]. In addition, systemic diseases associated with periodontal disease, *e.g.*, diabetes, cardiovascular and cerebrovascular diseases, pregnancy, osteoporosis, and Alzheimer's disease, endanger the physical and mental health of patients [4]. Although the progression of periodontal disease can be slowed down by reducing inflammation via mechanical plaque removal based on scaling, lesions resulting from bone loss, particularly that of the alveolar bone, are irreversible [5]. Therefore, improving repair and reconstruction methodologies of alveolar bone defects has remained a popular research topic in periodontal disease treatment.

With recent developments in material and biological sciences, the potential application of tissue engineering to bone regeneration, while also satisfying clinical requirements, has been investigated [6–8]. Recently, owing to the detailed study of mobilizable/homing endogenous resident stem cells and growth factors, endogenous tissue regeneration (ERM) has garnered tremendous attention in this field [9,10]. In relatively young patients, with active growth and metabolism and excellent function of endogenous stem cells, endogenous regeneration and repair is the preferred alternative [11]. Compared to treatments involving *in vitro* expansion of stem cells, ERM circumvents the complex processes involved in tissue engineering and thereby facilitates the development of clinically translatable regenerative approaches [12,13].

Numerous studies have demonstrated the advantages of cell- and growth factor-encapsulated hydrogel scaffolds in bone regeneration over the past decade [14,15]. They have been utilized as a platform to improve regenerative payload delivery owing to their unique physico-chemical properties, *e.g.*, their porosity and other mechanical properties are tuneable to site-specific tissue types [16,17]. Successful bone regeneration requires a complex and coordinated cascade of growth factors (GFs) and cells. Thus, designing a biomaterial capable of improving the stability and longevity of GFs, guiding stem cell homing, and promoting proper cell residency and differentiation simultaneously are crucial steps [18]. Further, a single GF cannot meet the requirements of periodontal tissue regeneration during the different stages—a combination of multiple GFs is required [19]. Our laboratory has been committed to the research of growth factors and their effects on osteogenic differentiation of human periodontal ligament stem cells (hPDLSCs) [20–22]. We have derived the following conclusions. (1) basic fibroblast growth factor (bFGF) can significantly promote the proliferation of mesenchymal stem cells (MSCs) and the formation of micro-vessels during early stages of bone regeneration. (2) transforming growth factor β3 (TGFβ3) facilitates osteogenic differentiation of hPDLSCs *in vitro*. Further, synthetically considering our previous studies and clinical requirements, we designed a dual-factor (bFGF and TGFβ3) sequentially releasing system to repair periodontal tissue defects.

In recent years, multiple biomaterial-based delivery systems have been developed to achieve controlled release of growth factors in bone tissue engineering [23]. The microsphere-gel scaffold structure is a widely used candidate owing to the simplicity of its method of preparation—the preparation environment needs to satisfy only a few conditions [15]. Further, it enables sequential release of different active ingredients with precise control over the release time and dosage [24]. In addition, the injectability and deformability of the microsphere-gel scaffold enables it to adapt to irregular bone defects. It is particularly suited to the narrow oral cavity [25]. An injectable hydrogel sulfated chitosan oligosaccharide was prepared in our laboratory, which is capable of effectively enhancing the biological activity of aFGF, enabling neuronal repair [26]. This motivated our goal of first encapsulating TGFβ3 in microspheres and then co-loading bFGF and TGFβ3-microspheres into a chitosan hydrogel. As the hydrogel degrades, the bFGF and microspheres in the hydrogel are preferentially released, followed by the delayed release of TGFβ3. This is analogous to the natural healing process, in which bFGF and TGFβ3 are released at different times to aid different stages of healing.

In summary, we fabricated a self-healing hydrogel system (DFH) consisting of TGFβ3-microspheres and bFGF to biologically mimic the micro-environment of alveolar bone defects. The effectiveness of DFH was evaluated both *in vitro* and *in vivo*. Based on the results, we expect it to be applied in the field of periodontal tissue engineering in the future.

2. Materials and methods

2.1. Materials

Chitosan was purchased from Zhejiang Jinke Pharmaceutical Co. Ltd. (Hangzhou, China). Chitosan-glutamate (CsGlu) was obtained from Wuhan Yuancheng Technology Development Co. Ltd. (Wuhan, China). 4-arm polyethylene glycol-
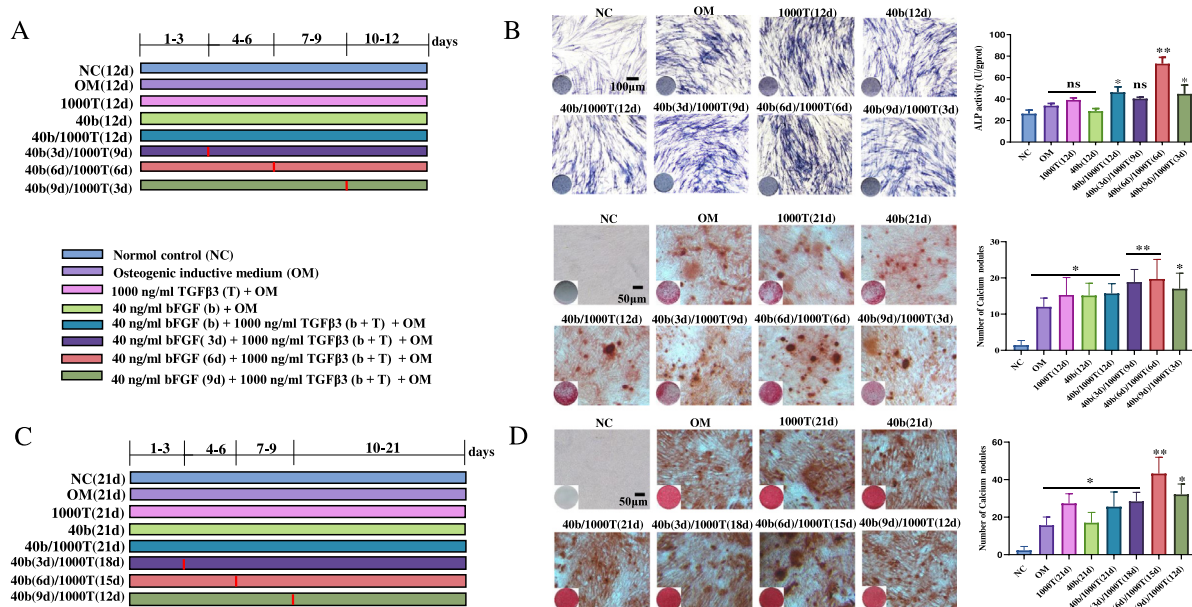
Fig. 1 – Sequential application of bFGF and TGFβ3 significantly increased ALP activity and mineral deposition in hPDLSCs. (A). Schematic diagram of sequential administration of bFGF and TGFβ3 (12 d). (B). After 12 d of culture, ALP staining and Alizarin red staining were performed. (C). Schematic diagram of sequential administration of bFGF and TGFβ3 (21d). (D). After 21 d of culture, Alizarin red staining was performed. ($n = 3$, *$P < 0.05$, **$P < 0.01$, vs. NC).

benzaldehyde (4Arm-PEG-DF) was purchased from Wuhu Ponsure Biological Technology Co. Ltd. (Wuhu, China). bFGF and TGFβ3 were provided by Jinan University Biopharmaceutical R&D Centre (Guangzhou, China). The enzyme-linked immunosorbent assay (ELISA) kits were purchased from Wuhan Huamei Biotechnology Co. Ltd. (Wuhan, China). hPDLSCs were obtained from our laboratory. ECV304-eGFP cells were purchased from the Chinese Academy of Sciences (Shanghai, China). All cell culture plates and bottles were obtained from Corning Company (Corning, NY).

2.2. The role of bFGF and TGFβ3 during the proliferation and differentiation of hPDLSCs

Sequential administration of bFGF and TGFβ3 was carried out following the revision presented in [27]. In brief, cells were seeded into 12-well plates and cultured in the following media for 12 or 21 d: basic medium (NC), osteogenic induction medium (OM), OM with 40 ng/ml bFGF, OM with 1000 ng/ml TGFβ3, OM with simultaneous application of bFGF and TGFβ3, and OM with 40 ng/ml bFGF pre-treated during the first 3/6/9 d and TGFβ3 during the remaining period. The experimental categories are depicted in Fig. 1A and 1C. After culturing for 12 or 21 d, the osteogenic differentiation of hPDLSCs was observed using ALP staining and Alizarin Red staining.

2.3. Preparation and characterization of DFH

DFH comprised two constituents—TGFβ3 chitosan microspheres (CMs) and bFGF self-healing hydrogel. The self-healing hydrogel was prepared by forming a Schiff base bond between the amine group on CsGlu and the active carbonyl group on 4Arm-PEG-DF. First, CMs were prepared

Table 1 – The gelation time of CsGlu and 4Arm-PEG-DF in different proportions.

Sample	CsGlu (w/v)	4Arm-PEG-DF (w/v)	Gel time (s)
1	1%	0.5%	~230
2	1%	1%	~105
3	1%	2%	~90
4	2%	0.5%	~110
5	2%	1%	~75
6	2%	2%	~65
7	3%	0.5%	~65
8	3%	1%	~40
9	3%	2%	~35

via emulsification and cross-linking (Fig. 2A). Next, CMs were incubated in TGFβ3 solution at 4 °C for 48 h to produce TGFβ3-loaded CMs. Then, TGFβ3-loaded CMs were added into the bFGF-CsGlu solution and mixed with the 4Arm-PEG-DF solution to obtain DFH.

2.4. Optimization and characterization of DFH

In order to optimize the composition of DFH, its gel time, scanning electron microscopy (SEM), rheological properties, and compression properties were recorded. Vial inversion method was used to determine its gelation times (Table 1). SEM (XL30, Philips, Germany) was used to observe its structure. A rotational rheometer (Kinexus Pro, Malvern) was used to measure the rheological properties of DFH. The reformation of DFH fragments into a whole was observed macroscopically to investigate the self-healing properties of DFH. Finally,
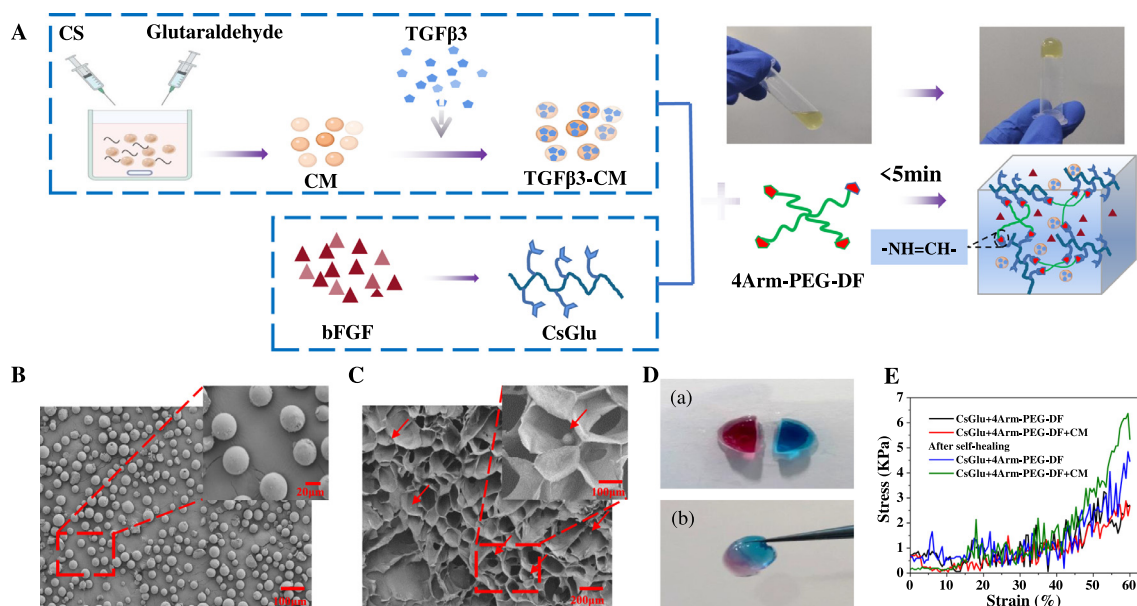
Fig. 2 – Preparation and characterization of DFH. **(A). Flow chart of TBFH preparation. (B). The morphology of CM was observed via SEM. (C). SEM observation of the structure of DFH and the microspheres in it. (D). Dyes of different colours were added to the DFH, chopped, and then combined to observe the self-healing process of the hydrogel. (E). Changes in mechanical properties of the DFH before and after self-healing.**

the dynamic universal testing machine (ELF3200, Bose, America) was used to evaluate the mechanical properties of DFH.

2.5.   In vitro degradation and release characteristics of DFH

The weight loss method was applied to evaluate degradation of DFH *in vitro*. The weighed (W_0) DFH was immersed in Phosphate Buffer Saline (PBS, pH 7.4) containing 20 µg/ml lysozyme, and continuously shaken in a constant temperature shaker at 37 °C. At predetermined times, portions of DFH were retrieved, its surface moisture was removed, and the DFH was weighed (W_t). The degradation rate (DR) of the gel was calculated using the following formula ($n = 3$):

$$DR\ (\%) = \frac{W_t}{W_0} \times 100$$

To ascertain the release profile, the release profile of bFGF and TGFβ3 from the DFH *in vitro* was evaluated by ELISA. The DFH were placed in the 12-well plates containing PBS (pH = 7.4) under the sustained oscillation. At predetermined intervals, 100 µl the supernatant was collected and evaluated with bFGF ELISA and TGFβ3 ELISA, followed by adding an equal volume of fresh PBS in well plates. Calculate the protein release rate and draw the cumulative release curve.

2.6.   Proliferation and osteogenic differentiation of cells in DFH

DFH and hPDLSCs (3×10^5 cells/well) were mixed and added to a 24-well plate. After culturing for 1, 3 and 7 d, the proportions

of living and dead cells were recorded via staining using Calcein-AM/PI living cell/dead cell double staining kit (Zeye Biotechnology Co. Ltd. Shanghai, China). To evaluate hPDLSCs osteogenesis differentiation, ALP staining was executed after culturing in the inducing medium for 7 d and 14 d.

2.7.   Promotion of tubule formation and cell migration by DFH in transwell

DFH (300 µl/well) was added to a 24-well plate to observe the tube-formation behaviour of human umbilical vein endothelial cells (HUVECs) (Shanghai, China) on DFH. Following the gelation of DFH, HUVECs with red fluorescence (1×10^5 cells/well) were added to the surface of the gel. After culturing for 24 h, the formation of the lumen was observed. Transwell migration assay was used to evaluate the ability of DFH to recruit MSCs. MSCs (5×10^4 cells/well) were seeded into the upper chamber of a Transwell (24-well) plate. DFH containing different concentrations of TGFβ3 was added to the lower chamber. After culturing for 48 h, it was stained with a crystal violet solution to measure the number of migrated cells.

2.8.   Animals

Specific-pathogen free male Sprague-Dawley (SD) rats (250 ± 20 g) with certificate no. 44007200069979 were supplied by the Guangdong Medical Laboratory Animal centre (Guangdong, China). They were kept in separate animal rooms at constant temperature (25 ± 2 °C) and humidity (55% $\pm$ 10%) on a 12-h light/dark cycle with free access to water and food. The experimental protocol was approved by the Ethics Review Committee for Animal Experimentation of

Table 2 – The group of *in vivo* recruitment of stem cells.

Groups		Gel composition
Control		blank hydrogel
bFGF		hydrogel with 80 ng/ml bFGF
TGFβ3		hydrogel with 1000 ng/ml TGFβ3
DFH	DFH-L	DFH with 80 ng/ml bFGF and 1000 ng/ml TGFβ3
	DFH–H	DFH with 80 ng/ml bFGF and 4000 ng/ml TGFβ3

Jinan University (ethical review no. 20200826–11), and all the experiments were conducted following the National Institutes of Health Guide for the Care and Use of Laboratory Animals (NIH Publications No. 8023, revised 1996).

2.9. DFH-induced recruitment of MSCs in the muscle pocket model of SD rats

As indicated by the categories presented in Table 2, DFH was implanted into the muscle pocket of SD rats to observe DFH-induced recruitment of MSCs *in vivo*. Each rat was injected with 100 μl DFH. The rats were euthanized seven d after the operation, and the gel and surrounding tissues were fixed with 4% paraformaldehyde and embedded in paraffin for histological sectioning. Following dewaxing and hydration, immunohistochemical analysis was performed on the sections to evaluate the expression of CD29 and CD45. Finally, the sections were dehydrated and sealed for microscopy.

2.10. DFH-induced repair of alveolar bone injury in SD rats

The experimental process of alveolar bone injury repair is depicted in Fig. 5**A**. After the rats were anesthetized (using 3% sodium pentobarbital), the left gingiva of the maxillary incisor of each rat was lacerated with a pointed scalpel to expose the surface of the alveolar bone. Then, a 1.5 mm diameter dental drill was used to drill a hole and create a spherical defect with a diameter of 2 mm and a depth of 1 mm.

One week after the operation, the periodontal defect was observed using Micro-CT and rats exhibiting unqualified alveolar bone defects were discarded. 24 animals were categorized in the following classes—Model group, Blank hydrogel group, DFH-L (DFH with 80 ng/ml bFGF and 1000 ng/ml TGFβ3), and DFH-H (DFH with 80 ng/ml bFGF and 4000 ng/ml TGFβ3). Each rat was injected with 100 μl DFH. The state of repair of the alveolar bones of these rats was observed after 12 weeks.

2.11. Quantitative real-time PCR

DFH scaffolds were retrieved after seven d. The total RNA of the tissue was extracted using the TRIzol reagent and reverse transcribed using the PrimeScript™-RT reagent kit (TaKaRa) by following the manufacturer's instructions. Real-time polymerase chain reaction (PCR) was performed using 2 × SYBR Green PCR Master Mix on a Real-Time PCR System. All the primer sequences were designed using the primer 5.0 software. The following primer sets were used: CD29—forward 5′-CTACTGGTCCCGACATCATC-3′ and reverse 5′-TGTCACGGCACTCTTGTAAA-3′; CD45—forward 5′-ACCACATATCTTCC AGGTGCC-3′ and reverse 5′-CCATTGGAGAGAGTGACGTTT-3′; and GAPDH—forward 5′- CTCTGCTCCTCCCTGTTCTA-3′ and reverse 5′-TCGTTGATGGCA ACAATGTC-3′. The relative expressions of CD29 and CD45 were calculated via the $2-\Delta\Delta$Ct method using GAPDH as a reference gene.

2.12. Histochemical staining

Briefly, alveolar bone tissue was fixed with 4% paraformaldehyde and embedded in paraffin for histological sectioning. Following dewaxing and hydration, the sections were examined using HE staining to analyse the formation of new bone. Masson's trichrome staining was utilised to further analyse the formation of collagen. The sections were analysed, and images were captured with a microscope (Olympus IX71; Tokyo, Japan).

2.13. Statistical analysis

All data are expressed as the mean ± standard deviation ($n = 3$). Statistical analyses were performed using the GraphPad Prism 6 software (GraphPad Software Inc., La Jolla, CA, USA). Differences between more than two groups were analysed using one-way ANOVA followed by Tukey's HSD comparison test. The threshold for statistical significance was set to be $P < 0.05$.

3. Results and discussion

3.1. Significant increase of ALP activity and mineral deposition in hPDLSCs by the sequential application of bFGF and TGFβ3

The sequential application of multiple GFs found in real-world biological processes is essential to periodontal regeneration. To validate the different functions of bFGF and TGFβ3 during the osteogenic differentiation of hPDLSCs, we designed an *in vitro* cell experiment by slightly altering the method of sequential administration [27]. As depicted in Fig. 1**B** and 1**D**, compared to the NC group, the combination of bFGF and TGFβ3 significantly enhanced the expression of ALP, with the performance of the 40b(6d)/1000T(6d) group being significantly better than those of others (**$P < 0.01$, *vs* NC). Pre-treatment with 40 ng/ml bFGF for 6 d, followed by that with 1000 ng/ml TGFβ3 for 6 to 18 d, produced the best mineralization promotion ability amongst all groups (**$P < 0.01$, *vs* NC). This indicates that bFGF pre-treatment for approximately 6 d, followed by TGFβ3 administration, significantly enhanced the osteogenic differentiation ability of hPDLSCs. Some studies have concluded that bFGF can activate endothelial cell proliferation and migration to promote angiogenesis through multiple signalling pathways [28]. However, although the establishment of the new vascular network is attributed to bFGF, subsequent creeping replacement of endogenous stem cells and new bone formation are attributed to TGFβ3 [29,30]. Ge et al. found

that bFGF exerts a time-dependant antagonistic effect on ALP activity induced by OM and BMP-2, while the sequential treatment of low-dose bFGF and BMP-2 can promote ALP activity in hPDLSCs [27]. In this study, we employed TGFβ3 instead of BMP2. TGFβ3 and BMP2 belong to the same family and are two classical growth factors involved in bone regeneration. Although TGFβ3 exhibits obvious advantages over BMP2 in terms of recruiting endogenous stem cells [31], TGFβ3 is still in the laboratory research stage due to the limitation of its industrialized amount. Our laboratory has overcome the difficulty of refolding recombinant human TGFβ3 and achieved large-scale production [32], but finer details of the plan are yet to be finalized.

3.2. Preparation, optimization, and characterization of DFH

Exogenous growth factors in periodontal tissues cannot fully exert their biological activities owing to their short half-life and fast diffusion rate. Therefore, it is necessary to design an appropriate system capable of controlling growth factors for therapeutic purposes. The proposed DFH system, composed of TGFβ3-microspheres and bFGF, is a promising candidate. The CM preparation process is depicted in Fig. 2A. The microspheres adsorbed TGFβ3 proteins owing to the combined effects of electrostatic properties and the internal pore structure. SEM revealed that the CMs were completely spherical with a particle size primarily distributed between 20 and 30 μm (Fig. 2B). Then, TGFβ3-microspheres were added into the bFGF-CsGlu solution, followed by the addition of 4Arm-PEG-DF. The mixed solution was gelled via Schiff-based bond formation within 5 min (Table 1). The optimized DFH composition was ascertained to be 2% CsGlu: 20% 4Arm-PEG-DF = 1:0.05 (v/v), with the concentration of microspheres being 5 mg/ml (**Fig. S1**).

DFH exhibits a layered porous structure with a porosity of approximately 84.3%, which lies within the porosity range of 50%–95% of natural alveolar bones, and a pore size between 100 and 300 μm, as observed via SEM. Numerous studies have established the requirement of good porosity and interconnected porous structures in engineered scaffolds that allow cells to attach and proliferate, thereby promoting angiogenesis, to mimic natural scaffold structures. The optimal range for pore size is 100–500 μm [15]. In this study, the prepared DFH exhibited a porosity of 84.3% and a pore size distribution between 100 and 300 μm. Thus, its structure is similar to that of healthy dense bone and favourable for bone regeneration (Fig. 2C).

In addition, as the resorption or injury of the alveolar bone in the oral cavity is usually an irregular wound, the ideal repair material should exhibit excellent plasticity and injectability. The self-healing property of DFH is that -NH2 on CsGlu and -CHO on 4Arm-PEG-DF react to form a Schiff base bond. We all know that the Schiff base bond is a reversible covalent bond, so the DFH gel prepared by the Schiff base reaction has the property of self-healing. At the same time, two pieces of gel of different colours were observed to splice together and aggregate into a single entity after 1 h, verifying the viability of the self-healing system (Fig. 2D). The mechanical compression test was performed on DFH before and after self-healing (Fig.

2E). The results established the constancy of the slope of the gel, which further proved the dynamic/reversible nature of the Schiff-based bonds. Based on the unique physicochemical properties of DFH, its application in tissue engineering is greatly broadened. Also, DFH degradation have a minor effect on the self-healing ability of the gel. In the self-healing ability test of DFH, we found that after the re-healed hydrogel was soaked in PBS buffer for 12 h, only the surface of the gel became less flat due to degradation.

3.3. In vitro release of bFGF and TGFβ3 in DFH

In the case of multivariate GFs, the order of release and the quantity introduced at each stage are important parameters to ensure the realization of the desired effect. The sequential release of the two proteins (1 ml DFH containing 80 ng bFGF and 1000 ng TGFβ3) was verified via in vitro release kinetic studies. The results (Fig. 3A) revealed that, during the initial stage, DFH swelled sufficiently in the PBS solution and started to dissolve rapidly. Alongside the morphologic change of DFH, bFGF was released rapidly, and the released proportion became 20% in 24 h. However, it was ensured via encapsulation that the released amount of TGFβ3 remained lower than the detection limit during this 24 h duration. Over time, the hydrogel gradually swelled sufficiently, and the cross-linked structure decelerated the dissolution of the gel. Then, bFGF was released slowly, with its proportion reaching 95% of the total amount after 168 h (7 d), when it was almost completely released. However, the released amount of TGFβ3 did not exceed the detection threshold until 36 h (4.60% ± 2.61%). At the end of the experiment (after 14 d), the released amount of TGFβ3 was observed to be 55% approximately. Thus, the viability of the proposed biomimetic binary delivery system was verified.

3.4. Microenvironment mimicked by DFH to promote tubule formation, induce cell migration, and aid osteogenic differentiation of hPDLSCs

The ability of DFH to promote microvascular formation and promote stem cell migration and differentiation in vitro was evaluated using Calcein-AM/PI staining, tubule formation assay, crystal violet staining, and ALP staining. As illustrated in Fig. 3B, hPDLSCs survived in the gel for more than 7 d After 24 h of culture, HUVECs formed tubular structures on DFH via ligation, migration, and differentiation. The tubular structures were particularly numerous and distinct in DFH containing 80 ng/ml bFGF (Fig. 4A). Further, in the Transwell cell migration assay Fig. 4B, the DFH group loaded with 250 ng/ml TGFβ3 recruited a higher number of cells compared to the other groups, indicating that DFH induced the migration of MSCs. In addition, the ALP staining of empty DFH was lighter, and the incorporation of TGFβ3 enhanced the pro-osteodifferentiation ability of DFH (Fig. 3C).

Cell-friendly biomaterials incorporate key physicochemical cues that can instruct and govern cell behaviour both in vitro and in vivo [33]. In this study, in order to simulate the spatial and temporal characteristics of a natural cellular environment, we incorporated bFGF and TGFβ3 within the hydrogel system—bFGF was incorporated
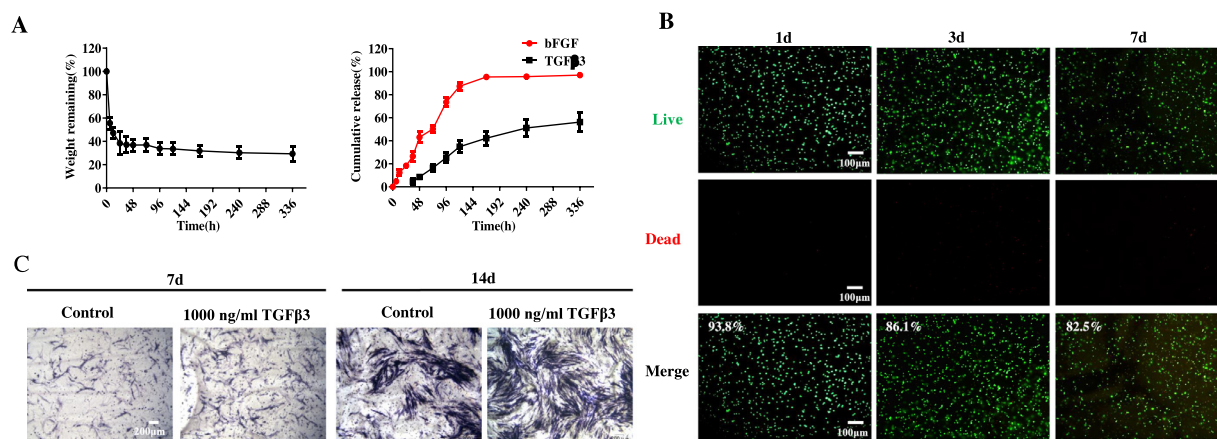
Fig. 3 – The release of GFs *in vitro* and the proliferation and osteogenic differentiation of hPDLSCs in DFH. **(A).** *In vitro* degradation and release curve of the DFH. **(B).** Surviving hPDLSCs in the DFH were observed via calcein-AM/PI staining, and the numbers of living and dead cells were counted using ImageJ ($n = 3$). **(C).** The DFH loaded with hPDLSCs was cultured in the osteogenic induction medium for 7 and 14 d and then stained with alkaline phosphatase.
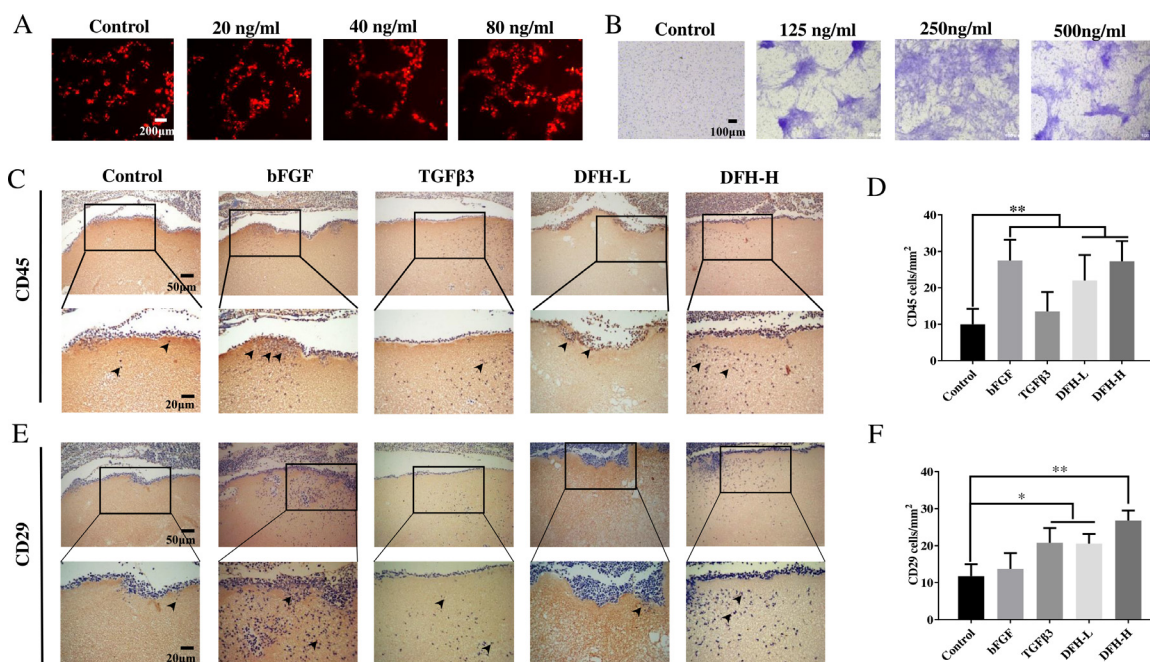

Fig. 4 – DFH mimics the microenvironment, promotes the formation of tiny blood vessels, and recruits MSCs *in vivo* and *in vitro*. **(A).** HUVECs were cultured in the DFH for 24 h. Tubular structures were observed using an immunofluorescence microscope. **(B).** HF-MSC migration was induced by the DFH. After 24 h of culture, the number of migrated stem cells was evaluated via crystal violet staining. **(C).** *In vivo* cell recruitment by the DFH. Immunohistochemistry of vascular endothelial cell marker CD45 and the MSC marker CD29 on the recruited cells. The black arrow indicates cell clusters with positive staining of CD29 or CD45. DFH-L: 80 ng/ml +1000 ng/ml TGFβ3; DFH−H: 80 ng/ml +4000 ng/ml TGFβ3. ($n = 3$, *$P < 0.05$, **$P < 0.01$, *vs* Control).

in the outer gel, which promoted the formation of new blood vessel network. The establishment of a new vascular network provided the requisite amount of oxygen and nutrients, and played a crucial role in removing waste products, laying the environmental foundation for new bone tissue. TGFβ3 was incorporated within the inner layer of microspheres, and its slow release not only guided the homing of stem cells but also guided the osteogenic differentiation of homing stem cells, thereby promoting complete regeneration of bone tissue.

3.5.   DFH-*induced promotion of the formation of tiny blood vessels and recruitment of MSCs in vivo*

The repair of natural bone tissue defects can be primarily divided into four stages—vascularization and cell recruitment, cell proliferation and differentiation, cartilage formation and hard bone tissue formation, and bone remodelling. Typically, the vascularization and cell homing process is completed within 5 d approximately [34,35].
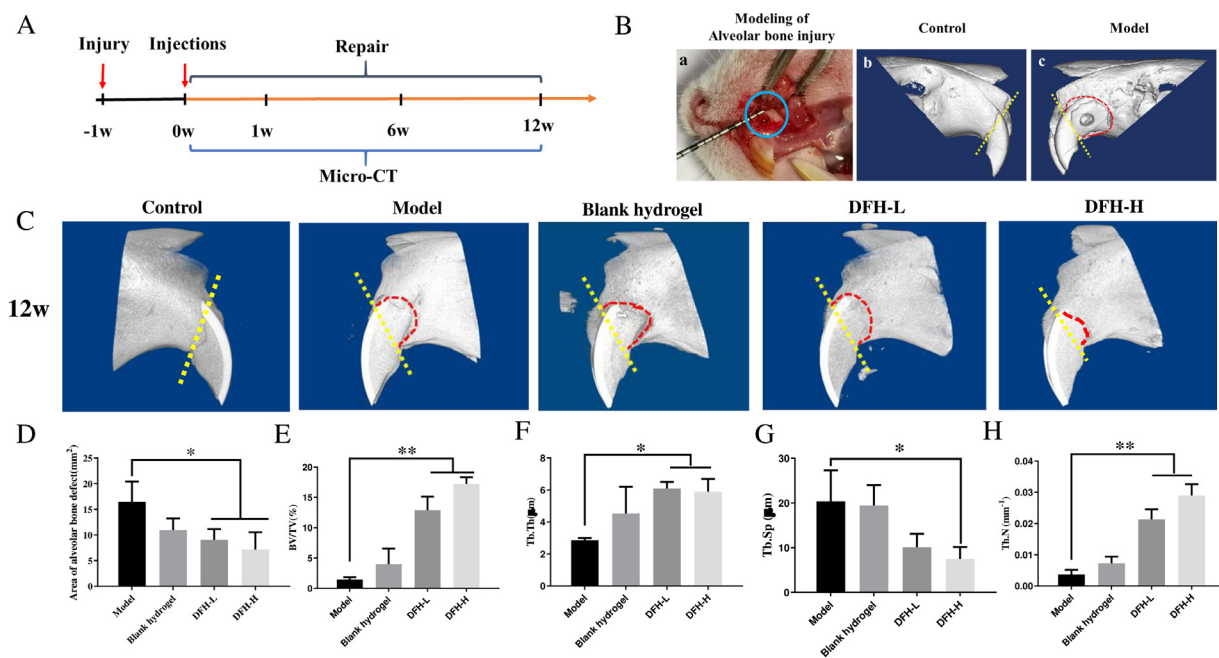
Fig. 5 – Repair of alveolar bone defects in SD rats. (A). Operational flow chart of alveolar bone injury repair. (B). The model of alveolar bone injury was established. One week later, the alveolar bone injury of rats was observed via Micro-CT. In the figure, the yellow dotted line indicates the location of the normal alveolar bone, and the red dotted line indicates the area of the injury. (C). After 12 weeks of administration, the alveolar bone repair states of different groups of DFH were observed via Micro-CT. (D). After 12 weeks of administration, the alveolar bone defect areas of different groups of DFH were calculated. (E-H). The volume fraction, trabecular number, trabecular separation, and trabecular thickness of the newly formed alveolar bone were analysed using the CTAn software ($n = 3$, *$P < 0.05$, **$P < 0.01$, vs Model).

Interestingly, the sequential dosing results described in Section 3.1 also corroborated better osteogenic differentiation ability of hPDLSCs following pre-treatment with bFGF for approximately 6 d before the administration of TGFβ3. The rat muscle pocket model was used to study the ability of DFH to promote microangiogenesis and recruit MSCs in $vivo$. Immunohistochemical analyses were performed to evaluate the expression of CD45 and CD29.

CD45 is a hematopoietic stem cell marker. As a fibronectin receptor, CD45 participates in multiple cell-cell and cell-matrix interactions, and regulates a variety of important biological functions. In this study, DFH groups were observed to exhibit more positive CD45 cells (*$P < 0.05$, vs both the blank and TGFβ3 group). Similarly, the number of positive cells in the bFGF group exhibited no statistical difference, which indicates that bFGF played an important role during angiogenesis (Figs. 4C and 4D). The expression of CD29 is positively correlated with the migration of MSCs. The number of CD29 positive cells around the materials both in DFH and TGFβ3 groups were significantly higher than in other groups (Figs. 4E and 4F, *$P < 0.05$). As illustrated in Fig. S4, the expression levels of CD29 and CD45 in the DFH-H group were significantly higher than those in the other groups. Yang et al. found that TGFβ3 helps bio-scaffolds to recruit IPFSCs in $vitro$ and supports cell settlement and chondrogenic differentiation of migratory cells [36]. This study established that TGFβ3 is the crucial component in DFH that aids the recruitment of MSCs both in $vivo$ and in $vitro$.

In short, DFH mimics the microenvironment of damaged tissue. It promotes the formation of tiny blood vessels and effectively recruits endogenous MSCs both in rat muscle pockets implanting expression and alveolar bone injuries in SD rats. The biocompatibility study revealed that DFH exhibits good biocompatibility in $vivo$ (**Fig. S3**).

3.6. Repair of alveolar bone injury by DFH in SD rats

Currently, research on stomatology tissue engineering is plagued by several problems—the lack of a satisfactory animal model is one of the foremost. In this study, the SD rat alveolar bone injury model was established by slightly revising the method outlined in [37] (the modelling method is described in Section 2.10). Micro-CT was utilised to investigate the changes in alveolar bone loss during the tests in $vivo$. The loss of alveolar bone in the model group increased over time, and it did not heal naturally in 12 weeks (Figs. 5B and 5C), which was confirmed by clinical dentists. Then, the proposed method was applied for subsequent experiments.

After 12 weeks of the operation, the alveolar bone defect in the blank gel group did not recover. Compared to the model and blank gel groups, DFH groups regenerated alveolar bone in the defective area, and the amount of new bone tissue in the DFH group were significantly higher than that in other groups (Fig. 5D). The bone volume fraction, trabecular number, and trabecular thickness of new bone (analysed using the CTAn

software) in DFH groups were significantly higher than those in the model and blank gel groups ($*P < 0.05$). The DFH-H group exhibited the best treatment effect (Figs. 5**E**–5**H**).

The regenerative tissue was studied in greater detail using HE and Masson's trichrome staining histological analyses (**Fig. S7**). HE staining of alveolar bone specimens at 12 weeks revealed the absence of any new bone formation at the defective sites in the model group and blank gel group. Bone resorption occurs at the bone defect site, with only a small amount of tissue fibre filling. New bone tissue in the DFH-H group was significantly greater than in other groups. The material in the bone defect was completely degraded, and a large amount of fibrous tissue was observed in the defect without any inflammatory cells. Masson staining revealed the low amount of blue fibrous tissue filling in the bone defect in the model and blank gel groups, with no obvious new bone formation. Compared to the model group, the DFH group, bFGF group and TGFβ3 group exhibited a large amount of blue fibrous tissue filling in the defect, with the undegraded material surrounded by blue fibrous tissue. New bone tissue was observed to have grown inwards from the edge of the bone defect. In summary, we successfully constructed a SD rat alveolar bone injury model. The model group were incapable of healing naturally. The DFH groups significantly promoted bone regeneration ($*P < 0.05$). The results verified the operational viability of the DFH hydrogel system.

For an active biological material, the ability to recruit stem cells *in vivo* is critical when the body is incapable of healing by itself. The proposed DFH hydrogel was verified to be capable of recruiting MSCs and repairing alveolar bone defects that are difficult to heal. The presence of DFH in alveolar bone defects promoted the formation of vascular networks and the expression of genes involved in the recruitment of MSCs confirms this view. Other studies have established that bFGF binds to FGFR receptors on the cell surface and activates VEGF-A to induce angiogenesis and provide necessary nutrients to injured sites. TGFβ3 plays a crucial role in guiding the migration and differentiation of MSCs. Pang et al. observed that TGFβ3 not only promotes the migration of hBMSCs directly through the TGFβ signalling pathway but also upregulates the secretion of MCP1 in vascular cells in a Smad3-dependant manner, thereby greatly enhancing the migration ability of TGFβ3 to hBMSCs [31]. In addition, TGFβ3 promotes the osteogenic differentiation of MSCs by activating the p38-MAPK pathway, thereby initiating bone regeneration [22]. However, most of the previous studies implemented a single growth factor or two simultaneous growth factors to promote tissue repair. In this study, a sequential drug delivery biomimetic carrier was constructed to further accelerate the repair of bone tissue by simulating the microenvironment of naturally damaged tissue. Although the sequential release system involving bFGF and BMP2 was reported by Ge et al., they did not publish any reports on the more complex case of animal experiments [27]. Besides, compared to BMP2, TGFβ3 not only promotes endochondral osteogenesis but also recruits endogenous stem cells. Therefore, we feel that this study expands the existing research and expect it to be helpful for future clinical use.

4. Conclusion

In this study, we simulated the inherent damage repair process of periodontal tissue and designed a self-repairing hydrogel system that releases bFGF and TGFβ3 sequentially. DFH is a porous (porosity: $84.3\% \pm 6.5\%$) hydrogel with good injectability and self-healing properties. Therefore, it is convenient for injection and administration in the narrow oral cavity. In addition, it has been established via gel-loaded cell experiments that DFH not only promotes tube formation by HUVECs and recruitment of MSCs but also promotes the osteogenic differentiation of hPDLSCs. We also successfully established a modified SD rat model of alveolar bone defect. After 12 weeks of *in situ* injection of DFH into the alveolar bone defect, it was found that the DFH group promoted the repair of the alveolar bone injury to a much greater extent than the control group. In summary, DFH was verified to exhibit good bone repair capability. As it is convenient for injection and administration in the narrow oral cavity, it can be expected to be used in clinical practice.

Conflicts of interest

The authors report no conflicts of interest. The authors are responsible for the content and writing of this paper.

Acknowledgments

Supplementary materials

Supplementary material associated with this article can be found, in the online version, at doi:10.1016/j.ajps.2022.03.003.

REFERENCE

[1] Nazir MA. Prevalence of periodontal disease, its association with systemic diseases and prevention. Int J Health Sci 2017;11(2):72–80.

[2] Ebersole JL, Graves CL, Gonzalez OA, Dawson D III, Morford LA, Huja PE, et al. Aging, inflammation, immunity and periodontal disease. Periodontology 2016;72(1):54–75.

[3] Frencken JE, Sharma P, Stenhouse L, Green D, Laverty D, Dietrich T. Global epidemiology of dental caries and severe

periodontitis - a comprehensive review. J Clin Periodontol 2017;44:S94–105.

[4] Williams RC, Barnett AH, Claffey N, Davis M, Gadsby R, Kellett M, et al. The potential impact of periodontal disease on general health: a consensus view. Curr Med Res Opin 2008;24(6):1635–43.

[5] Michaud DS, Fu Z, Shi J, Chung M. Periodontal disease, tooth loss, and cancer risk. Epidemiol Rev 2017;39(1):49–58.

[6] Zhao D, Zhu T, Li J, Cui L, Zhang Z, Zhuang X, et al. Poly(lactic-co-glycolic acid)-based composite bone-substitute materials. Bioact Mater 2021;6(2):346–60.

[7] Yang R, Chen F, Guo J, Zhou D, Luan S. Recent advances in polymeric biomaterials-based gene delivery for cartilage repair. Bioact Mater 2020;5(4):990–1003.

[8] Zhou J, Zhang Z, Joseph J, Zhang X, Ferdows BE, Patel DN, et al. Biomaterials and nanomedicine for bone regeneration: progress and future prospects. Exploration 2021;1(2):20210011.

[9] Yin Y, Li X, He XT, Wu RX, Sun HH, Chen FM. Leveraging stem cell homing for therapeutic regeneration. J Dent Res 2017;96(6):601–9.

[10] Wu RX, Yin Y, He XT, Li X, Chen FM. Engineering a cell home for stem cell homing and accommodation. Advanced Biosystems 2017;1(4):1–35.

[11] Wells JM, Watt FM. Diverse mechanisms for endogenous regeneration and repair in mammalian organs. Nature 2018;557(7705):322–8.

[12] Wu RX, Xu XY, Wang J, He XT, Sun HH, et al. Biomaterials for endogenous regenerative medicine: coaxing stem cell homing and beyond. Appl Mater Today 2018;11:144–65.

[13] Xu XY, Li X, Wang J, He XT, Sun HH, Chen FM. Concise review: periodontal tissue regeneration using stem cells: strategies and translational considerations. Stem Cells Transl Med 2019;8(4):392–403.

[14] Censi R, Martino PD, Vermonden T, Hennink WE. Hydrogels for protein delivery in tissue engineering. J Control Release 2012;161(2):680–92.

[15] Zhu T, Cui Y, Zhang M, Zhao D, Liu G, Ding J. Engineered three-dimensional scaffolds for enhanced bone regeneration in osteonecrosis. Bioact Mater 2020;5(3):584–601.

[16] Naahidi S, Jafari M, Logan M, Wang Y, Yuan Y, Bae H, et al. Biocompatibility of hydrogel-based scaffolds for tissue engineering applications. Biotechnol Adv 2017;35(5):530–44.

[17] Liu H, Xiang X, Huang J, Zhu B, Wang L, Tang Y, et al. Ultrasound augmenting injectable chemotaxis hydrogel for articular cartilage repair in osteoarthritis. Chinese Chemical Letters 2021;32(5):1759–64.

[18] Pacelli S, Basu S, Whitlow J, Chakravarti A, Acosta F, Varshney A, et al. Strategies to develop endogenous stem cell-recruiting bioactive materials for tissue repair and regeneration. Adv Drug Deliv Rev 2017;120:50–70.

[19] Newman MR, Benoit DS. Local and targeted drug delivery for bone regeneration. Curr Opin Biotechnol 2016;40:125–32.

[20] Li Y, Yu F, Liu Y, Liang Q, Huang Y, Xiang Q, et al. Sulfonated chitosan oligosaccharide alleviates the inhibitory effect of basic fibroblast growth factor on osteogenic differentiation of human periodontal ligament stem cells. J Periodontol 2019;91(7):975–85.

[21] Huang S, Yu F, Cheng Y, Li Y, Chen Y, Tang J, et al. Transforming growth factor-beta3/recombinant human-like collagen/chitosan freeze-dried sponge primed with human periodontal ligament stem cells promotes bone regeneration in calvarial defect rats. Front Pharmacol 2021;12:1–11.

[22] Li Y, Qiao Z, Yu F, et al. Transforming growth factor-beta3/chitosan sponge (TGF-beta3/CS) facilitates osteogenic differentiation of human periodontal ligament stem cells. Int J Mol Sci 2019;20(20):1–14.

[23] Wubneh A, Tsekoura EK, Ayranci C, Uludağ H. Current state of fabrication technologies and materials for bone tissue engineering. Acta Biomater 2018;80:1–30.

[24] Jeong HJ, Gwak SJ, Seo KD, Lee S, Yun JH, Cho YS, et al. Fabrication of Three-Dimensional Composite Scaffold for Simultaneous Alveolar Bone Regeneration in Dental Implant Installation. Int J Mol Sci 2020;21(5):1–11.

[25] He XT, Li X, Xia Y, Yin Y, Wu RX, Sun HH, et al. Building capacity for macrophage modulation and stem cell recruitment in high-stiffness hydrogels for complex periodontal regeneration: experimental studies in vitro and in rats. Acta Biomater 2019;88:162–80.

[26] Liu Y, Yu F, Zhang B, Zhou M, Bei Y, Zhang Y, et al. Improving the protective effects of aFGF for peripheral nerve injury repair using sulfated chitooligosaccharides. Asian J Pharm Sci 2019;14(5):511–20.

[27] Kang W, Liang Q, Du L, Shang L, Wang T, Ge S. Sequential application of bFGF and BMP-2 facilitates osteogenic differentiation of human periodontal ligament stem cells. J Periodontal Res 2019;54(4):424–34.

[28] Hao W, Han J, Chu Y, Huang L, Zhuang Y, Sun J, et al. Collagen/Heparin bi-affinity multilayer modified collagen scaffolds for controlled bFGF release to improve angiogenesis in vivo. Macromol Biosci 2018;18(11): e1800086.

[29] Ogawa K, Miyaji H, Kato A, Kosen Y, Momose T, Yoshida T, et al. Periodontal tissue engineering by nano beta-tricalcium phosphate scaffold and fibroblast growth factor-2 in one-wall infrabony defects of dogs. J Periodontal Res 2016;51(6):758–67.

[30] Ripamonti U. Redefining the induction of periodontal tissue regeneration in primates by the osteogenic proteins of the transforming growth factor-beta supergene family. J Periodontal Res 2016;51(6):699–715.

[31] Deng M, Mei T, Hou T, Luo K, Luo F, Yang A, et al. TGFβ3 recruits endogenous mesenchymal stem cells to initiate bone regeneration. Stem Cell Res Ther 2017;8(1):1–12.

[32] Zhou M, Shi W, Yu F, Zhang Y, Yu B, Tang J, et al. Pilot-scale expression, purification, and bioactivity of recombinant human TGF-beta3 from Escherichia coli. Eur J Pharm Sci 2019;127:225–32.

[33] Zhang Y, Liu X, Zeng L, Zhang J, Zuo J, Zou J, et al. Polymer fiber scaffolds for bone and cartilage tissue engineering. Adv Funct Mater 2019;29(36):1903279.

[34] Cai L, Lin D, Chai Y, Yuan Y, Liu C. MBG scaffolds containing chitosan microspheres for binary delivery of IL-8 and BMP-2 for bone regeneration. J Mater Chem B 2018;6(27):4453–65.

[35] Chen FM, Zhang J, Zhang M, An Y, Chen F, Wu ZF. A review on endogenous regenerative technology in periodontal regenerative medicine. Biomaterials 2010;31(31):7892–927.

[36] Yang Z, Li H, Tian Y, Fu L, Gao C, Zhao T, et al. Biofunctionalized structure and ingredient mimicking scaffolds achieving recruitment and chondrogenesis for staged cartilage regeneration. Front Cell Dev Biol 2021;9:1–17.

[37] Sowmya S, Mony U, Jayachandran P, Reshma S, Kumar RA, Arzate H, et al. Tri-layered nanocomposite hydrogel scaffold for the concurrent regeneration of cementum, periodontal ligament, and alveolar bone. Adv Healthc Mater 2017;6(7):1–13.